RESEARCH ARTICLE

Spatial distribution of N-cycling microbial communities showed complex patterns in constructed wetland sediments

David Correa-Galeote[1], Diana E. Marco[1,2], Germán Tortosa[1], David Bru[3], Laurent Philippot[3] & Eulogio J. Bedmar[1]

[1]Department of Soil Microbiology and Symbiotic Systems, Estación Experimental del Zaidín, Agencia CSIC, Granada, Spain; [2]Facultad de Ciencias Agropecuarias, Universidad Nacional de Córdoba, and CONICET, Ciudad Universitaria, Córdoba, Argentina; and [3]INRA-Université de Bourgogne, UMR 1229, Microbiologie et Géochimie des Sols, Dijon Cedex, France

Correspondence: Diana E. Marco, Facultad de Ciencias Agropecuarias, Universidad Nacional de Córdoba, and CONICET, Ciudad Universitaria, CC 509, 5000 Córdoba, Argentina. Tel.: +54 3543 493183; fax: +54 3543 493184; e-mail: dmarco@agro.unc.edu.ar

Received 3 May 2012; revised 30 July 2012; accepted 14 August 2012.
Final version published online 24 September 2012.

DOI: 10.1111/j.1574-6941.2012.01479.x

Editor: Tillmann Lueders

Keywords
constructed wetlands; N-cycling microbes; spatial patterns.

Abstract

Constructed wetlands are used for biological treatment of wastewater from agricultural lands carrying pollutants such as nitrates. Nitrogen removal in wetlands occurs from direct assimilation by plants and through microbial nitrification and denitrification. We investigated the spatial distribution of N-cycling microbial communities and genes involved in nitrification and denitrification in constructed wetland sediments receiving irrigation water. We used quantitative real-time PCR (qPCR) to characterize microbial communities. Geostatistical variance analysis was used to relate them with vegetation cover and biogeochemical sediment properties. The spatial distribution of the N-cycling microbial communities of sediments was heterogeneous and complex. Total communities of bacteria and crenarchaea showed different spatial distributions. Analysis of autocorrelation patterns through semivariance indicated a tendency towards a patchy distribution over scales around 10 m for genes involved in the nitrification and denitrification processes. In contrast, biogeochemical sediment properties showed diverse spatial distributions. While almost no patchiness was found for pH and moisture, patchiness at scales between 8 and 10 m was detected for carbon, nitrate and ammonia. Denitrification variables showed spatial autocorrelation at scales comparable to genes. However, denitrifying enzyme activity and potential N_2O production showed a common spatial pattern, different from that of the $N_2O/(N_2O + N_2)$.

Introduction

Nitrogen (N) is one of the most important plant nutrients in terrestrial ecosystems, but excess use of reactive nitrogen threatens the quality of air, soil and water (Rockström *et al.*, 2009). Thus, more than 11 million tonnes of N fertilizers are used in EU agricultural and much of this added N is lost in the environment (Sutton *et al.*, 2011). For example, the nitrate leaching from crops in Spain may reach to 150–300 N kg ha^{-1} (Ramos *et al.*, 2002). When nitrate ends up in water, it contributes to eutrophication, the excessive growth of algae that causes the death of other organisms such as fishes. High levels of nitrate in drinking water are also of human health concerns because it can poison infants by provoking methemoglobinemia (Greer & Shannon, 2005). In addition, nitrate can be transformed in the digestive tract in nitrosamines, which are carcinogenic (Craddock & Henderson, 1986). Constructed wetlands have been extensively developed in the last decades as alternatives to on-site treatment methods for diffuse or nonpoint nitrogen pollution of water and are used for biological treatment of wastewater from agricultural lands, industries or medium-size urban settlements (Leonard & Swanson, 2001; Bruland *et al.*, 2006). Nitrogen removal in constructed wetlands varied between 250 and 603 g N m^{-2} $year^{-1}$ (Vymazal, 2011). Apart from direct assimilation by plants, removal of N is achieved through microbial nitrification (Purkhold *et al.*, 2000; Treusch *et al.*, 2005) and denitrification activities (Hey *et al.*, 2012). These two N-cycling processes are mainly associated with the subsurface sediment (Kallner Bastviken *et al.*, 2003). For a better management

of constructed wetlands, the role of plant species, pH, nutrient flow and organic carbon availability have mostly been investigated (Bachand and Horne, 2000; Park *et al.*, 2008; Peralta *et al.*, 2010).

Despite their crucial role in N-removal, only few studies have focused on the microorganisms performing the nitrification and denitrification processes in constructed wetlands (Song *et al.*, 2010, 2012; Chon *et al.*, 2011). Analysis of the potential activity and the diversity of nitrifying and denitrifying communities in constructed wetlands show that plants species influence both the functioning and structure of these N-cycling guilds (Ruiz-Rueda *et al.*, 2008). Similarly, the presence and type of plants was related to the abundances of denitrifiers in the same wetland (Garcia-Lledó *et al.*, 2011). Differences in the denitrifier community structure were also reported between the different areas of the wetland sediment by Kjellin *et al.* (2007). The microbial community structure patterns were related to the water flow showing increased diversity with decreasing nutrient levels and increasing water residence times. The water residence times also best explained spatial variations of potential denitrification in the wetland (Kjellin *et al.* 2007). While the spatial distribution of N-cycling communities has been investigated in arable soil for a better understanding of N-processes in soil (Philippot *et al.*, 2009a; Enwall *et al.*, 2010), our knowledge the spatial distribution of the different microbial guilds in constructed wetlands is scarce. However, understanding the spatial heterogeneity of the nitrifying and denitrifying communities and of their activities across these engineered systems in relation to biogeochemical sediment properties and vegetation cover is of importance for wetland construction and optimal N-removal.

In this work, we investigated the spatial distribution of the abundance and the activity of N-cycling microbial guilds in constructed wetland sediments receiving irrigation water from orchard crops. As the irrigation water course through the constructed wetland was expected to cause spatial variation in nitrogenated leachates, we hypothesized that key environmental variables, potential denitrification, potential N_2 O emissions and communities of microbial denitrifiers and ammonia oxidizers would show a defined spatial structure. Microbial communities were quantified by real-time PCR and along with environmental and denitrification measurements were analysed using geostatistical methods.

Material and methods

Experimental site

The experimental site was a constructed wetland called Los Guayules (UTM coordinates 29S 0721735, 4108590) located near El Rocio marsh within Doñana National Park (south-west Spain). The wetland receives water from irrigation of nearby fruit orchards. The water regime is seasonal, flooding in winter and partially drying during summer. Vegetation is represented by a perennial community of aquatic and water-associated plants dominated by *Typha* spp., *Imperata cylindrica*, *Juncus effusus*, *Scirpus holoschoenus* and *S. maritimus* (Supporting information, Fig. S1a).

Sampling design

To detect the spatial variation of environmental variables, denitrifying genes and associated activity, a regular design of 50 sampling points in a 25 × 50 m grid with 5 m separation distance was used. The grid was oriented following the irrigation water course through the constructed wetland (Fig. S1b). Sampling was carried out during the dry season. The dry season was chosen for sampling because it was the time when a higher abundance of denitrifiers was found, determined by qPCR in preliminary surveys. The wetland sediments remain with high moisture content even during the dry season. Vegetation cover was estimated by recording the percentage of cover using a 25 × 25 cm square placed over each sampling point. Cover percentage was coded as 0 (no vegetation cover), 1 (1–50% cover), 2 (51–75% cover) and 3 (75–100%) cover.

Soil analyses

Texture of the site sediments was determined in samples according to the Spanish Official Methods for Soils and Waters (MAPA, 1974). It was classified as sandy clay loam sediment and contains 55% sand, 22.5% clay and 22.5% silt.

The top sediment layer (0–20 cm) was collected from the 50 sampling points. Samples were kept refrigerated during transport to the laboratory. Samples were appropriately fractionated, either immediately treated or stored under appropriate conditions depending on the analyses to be performed. Sediment moisture was determined gravimetrically by over-drying the sample at 105 °C for 24 h. In fresh samples, NH_4^+ (after 2 h extraction 1 : 20 w/v with 2N KCl), NO_3^- and NO_2^- (water-extracted 1 : 20 w/v) and pH (after water extraction 1 : 5 w/v for 2 h), total organic carbon (TOC) and total nitrogen (TN) were determined as indicated earlier (Tortosa *et al.*, 2011).

Denitrification activity measurements

Potential denitrifying enzyme activity (DEA) was determined in fresh sediment samples using an acetylene inhibition technique as previously described (Ryden &

Dawson, 1982). Briefly, anaerobic slurry was prepared by mixing 25 g soil and 25 mL of a solution containing 1 mM glucose, 1 mM KNO_3 and 1 g L^{-1} chloramphenicol in a 125-mL glass bottle. The headspace was evacuated and flushed four times with He and 10 mL of acetylene were added. The samples were shaken at 25 °C, and the concentration of N_2O was measured in the headspace after 30 and 60 min of incubation by gas chromatography as previously described (Tortosa *et al.*, 2011). DEA was calculated from the N_2O increase during incubation using the Bunsen coefficient for the N_2O dissolved in water. Potential N_2O production was determined by incubating parallel sediment samples without acetylene.

DNA extraction

DNA was extracted from 250 mg of each sub-sample stored at −80 °C according to the ISO standard 11063 'Soil quality-Method to directly extract DNA from soil samples' (Petric *et al.*, 2011). Briefly, samples were homogenized in 1 mL of extraction buffer (1 M Tris–HCl, 0,5 M EDTA, 1 M NaCl, 20% PVP 40, 20% SDS) for 30 s at 1600 r.p.m. in a minibead beater cell disrupter (Mikro-DismembratorS; B. Braun Biotech International). Soil and cell debris were removed by centrifugation (14 000 ***g*** for 1 min at 4 °C). After precipitation with ice-cold isopropanol, nucleic acids were purified using both PVPP (Biorad) and GeneClean (MP Bio) spin columns. Quality and size of soil DNAs were checked by electrophoresis on 1% agarose. DNA was also quantified by spectrophotometry at 260 nm using a BioPhotometer (Eppendorf, Hamburg, Germany).

Quantification of the N-cycle-associated microbial community

The size of the nitrifier community was estimated by quantitative PCR (qPCR) of *amoA* from ammonia-oxidizing bacteria (AOB) and archaea (AOA) (Wessén *et al.*, 2011) and that of the denitrifier community by qPCR of *narG*, *napA*, *nirK*, *nirS* and *nosZ* gene fragments using reaction mixtures, primers and thermal cycling conditions described previously (Henry *et al.*, 2004, 2006; Kandeler *et al.*, 2006; Bru *et al.*, 2007; Philippot *et al.*, 2009a, b). The total bacterial and crenarchaeal community was quantified using 16S rRNA gene as molecular marker as described by Lopez-Gutiérrez *et al.* (2004) and Ochsenreiter *et al.* (2003), respectively. Reactions were carried out in an ABI Prism 7900 Sequence Detection System (Applied Biosystems). Quantification was based on the fluorescence intensity of the SYBR Green dye during amplification. Two independent qPCR assays were performed for each gene. Standard curves were obtained using serial dilutions of linearized plasmids containing cloned *amoA*, *narG*, *napA*, *nirK*, *nirS*, *nosZ* and 16S rRNA genes amplified from bacterial strains. PCR efficiency for the different assays ranged between 90% and 99%. No template controls gave null or negligible values. Presence of PCR inhibitors in DNA extracted from soil was estimated by (i) diluting soil DNA extract and (ii) mixing a known amount of standard DNA to soil DNA extract prior to qPCR. In all cases, inhibition was not detected. Methodological evaluation of the real-time PCR assays showed a good reproducibility of 95.0 ± 12% between two runs.

Statistical analysis

Variables includes in the study were explored using standard statistical techniques. Many of the variables did not meet the normality assumptions and thus several transformation procedures were applied. Correlations (either parametric or nonparametric) were performed on transformed variables. Statistical analyses were performed using SPSS 18 (IBM). Spatial analyses (Cressie, 1991) were performed with transformed variables using semivariograms models from GS+ 9 (GAMMA DESIGN Software). Semivariance is a statistic measuring the degree of autocorrelation between spatial samples at different lag distances; in other words, it calculates the degree of similarity between points on a surface. Spatial analyses (Cressie, 1991) were performed with transformed variables using semivariograms models from GS+ 9 (GAMMA DESIGN Software). Semivariance is a statistic measuring the degree of autocorrelation between spatial samples at different lag distances:

$$\gamma(h) = [1/2\mathrm{N}(h)] \sum [z_i - z_{i+h}]^2$$

where γ (h) = semivariance for interval distance class h; z_i = measured sample value at point i; z_{i+h} = measured sample value at point $i + h$; and $\mathrm{N}(h)$ = total number of sample couples for the lag interval h.

Semivariograms are characterized by three model parameters: nugget variance, model y intercept; sill, model asymptote; range, distance over which spatial correlation is apparent. For linear semivariograms, there is no sill and no effective range, because spatial autocorrelation occurs throughout the entire range sampled and there is no characteristic spatial scale for variation. For exponential and Gaussian models, the range is the distance at which the sill $(C + C_0)$ is within 5% of the asymptote (the sill never meets the asymptote in these models). Semivariance fit: residual sum of squares (RSS), $[C/(C_0 + C)]$: proportion of sample variance $(C_0 + C)$ that is explained by spatially structured variance C (0 = pure nugget effect). Semivariograms were calculated

with the field data and fitted to any of the following models: linear, exponential, spherical or Gaussian, either isotropic or anisotropic, using the statistics (RSS, the residual sums of squares and $C_0/(C_0 + C)$, the proportion of sample variance $(C_0 + C)$ that is explained by spatially structured variance C) provided by the software. RSS provides an exact measure of how well the model fits the data; the lower RSS, the better the model fits. Thus, from different possible models, the one with lower RSS is chosen. $C_0/(C_0 + C)$ value will be 1.0 for a variogram with no nugget variance (where the curve passes through the origin); conversely, it will be 0 where there is no spatially dependent variation at the range specified, that is, where there is a pure nugget effect. This pure nugget effect should be interpreted with caution because it may be the result of a lack of resolution at small spatial scales. Fractal variograms were also calculated to explore if the measured variables showed fractal or self-similarity properties, indicated by the Hausdorff-Besicovitch statistic *D* (Burrough 1981). *D* is close to 1 for linear dimensions and 2 for plane dimensions.

Interpolation to estimate values in an area for points not actually sampled was carried out by ordinary kriging over the whole sampled field. Cross-validation analysis was used to evaluate kriging fit. In cross-validation analysis, each measured point in the spatial domain is individually removed from the domain and its value estimated as though it were never there. Then, the point is replaced, and the next point is removed and estimated, and so on. In this way, a regression of estimated vs. actual values for each sample location in the domain is calculated. The regression coefficient represents a measure of the goodness of fit for the least-squares model describing the linear regression equation. A perfect 1 : 1 fit would have a regression coefficient (slope) of 1.00.

For more details on geostatistical methods refer to the Appendix S1.

Gene abundances were analysed as absolute or relative abundances (gene copy number/16S rRNA gene Bacteria copy number). As the number of 16S rRNA gene operon per cells is variable (Klappenbach *et al.*, 2001), we did not convert the 16S rRNA gene copy data into cells numbers and we expressed our results as gene copy numbers per nanogram of DNA. Calculation of the gene copy number per nanogram of DNA instead of gram of soil minimized any bias related to soil DNA extraction efficiency.

Results

Environmental variables

The sampled area was almost totally covered with vegetation, although with different percentages (Fig. S2). The surveyed sediment was acid, with pH values ranging from 4.47 to 6.42. Percentage of sediment moisture varied from 3.53 to 22.46. Total organic carbon (TOC) varied from 2.91 to 23.35 g kg^{-1} dry sediment. Ammonium and NO_3^- content varied widely, up to 8.73 and 168 mg kg^{-1} dry sediment respectively, depending on the vicinity to the source of suspected contaminated water. Total nitrogen (TN) content varied less, ranging from 0.24 to 1.89 g kg^{-1} dry sediment. Expectedly, several sediment variables were cross-correlated (Table S1). NO_3^- was correlated with TN content and TOC. TN showed a high correlation with TOC, a lower one with sediment moisture and an inverse correlation with pH. Sediment moisture was also correlated with TOC and inversely correlated with pH. Only pH was significantly correlated (negatively) with vegetation cover and ammonia.

Fitted semivariance models revealed that sediment pH (Fig. 1, Table S2) and moisture (Table S2) showed spatial dependence over almost all the range considered (ranges about 31 m). In contrast, TOC (Table S2), NO_3^- and ammonia (Table S2 and Fig. 1) did not show spatial dependence over medium and larger scales (ranges between 8 and 10 m). As TN was fitted by a linear semivariance model, no spatial dependence was observed at the scale considered in the study (pure nugget effect) (Table S2 and Fig. 1).

Fractal variograms showed values of the Hausdorff-Besicovitch statistic *D* close to 2, indicating a plane distribution of self-similar, repetitive variation of the environmental variables over the sampled area, but only sediment moisture and ammonia showed good fit ($R^2 = 0.88$ and 0.56, respectively, Table S3). In contrast, nitrate concentration showed a *D* value closer to 1.5 ($R^2 = 0.49$), indicating a repetitive but more linear distribution (Table S3). Interpolated (kriged) maps of environmental variables showed a good fit, except for nitrate (Table S3). Spatial distribution of environmental variables is shown in Fig. 2 and Fig. S3.

Spatial distribution of microbial communities

Gene abundances were analysed as absolute (hereafter abundance) or relative abundances (gene copy numbers/16S rRNA gene Bacteria copy numbers, hereafter relative abundance). Abundances of both total bacterial and crenarchaeal community (16S rRNA gene of Bacteria and crenarchaea) and denitrification genes (*narG*, *napA*, *nirS*, *nirK*, *nosZ*) were highly variable, ranging several magnitude orders. Absolute abundance of 16S rRNA gene of Bacteria ranged between 360 and 360 000 copies, one order of magnitude greater than the number of copies of 16S rRNA gene of crenarchaea. The *narG* absolute abundance varied between 30 and 5700 copies, one order of

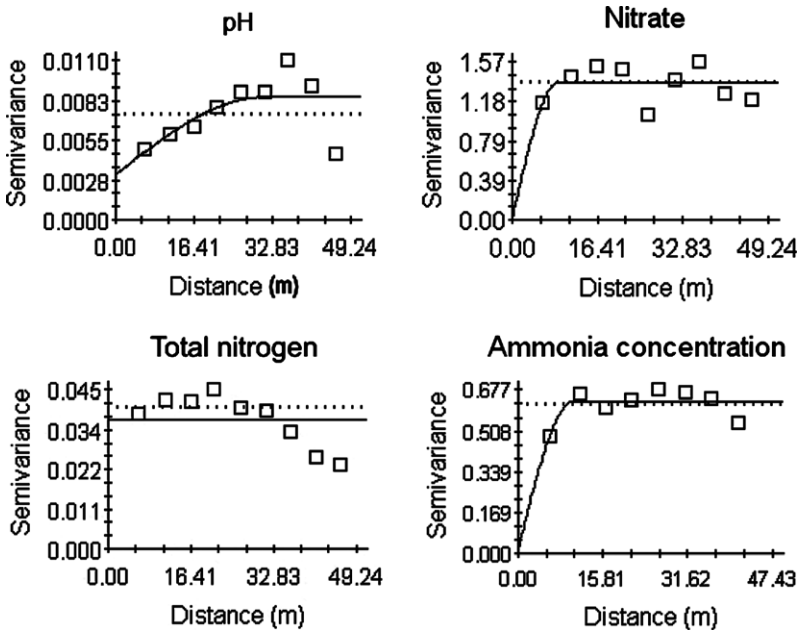

Fig. 1. Semivariograms of some environmental variables. Semivariance models and parameters for all the environmental variables are given in Table S2.

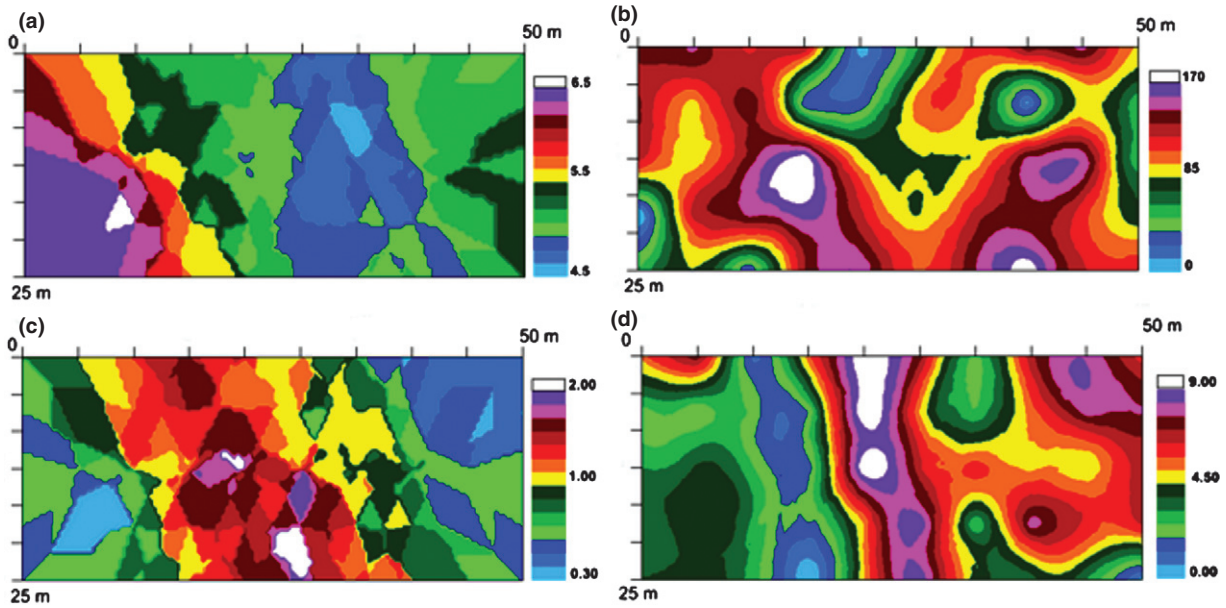

Fig. 2. Interpolated maps for environmental variables. (a) pH, (b) nitrate (mg kg^{-1} sediment), (c) total nitrogen (g kg^{-1} sediment) and (d) ammonia (mg kg^{-1} sediment). Colour scales indicate extrapolated values by kriging. Maps are shown in the same orientation as in Fig. S1b (sampling area).

magnitude lower than *napA*. *nirK* absolute abundance ranged between 4 and 3700 copies, one order of magnitudes lower than *nirS*. *nosZ* varied between 10 and 1700 copies. In general, abundances of *narG*, *napA*, *nirS-nirK* were highly correlated with total bacterial community (as determined by the 16Sr RNA gene) (Spearman's rho values between 0.85 and 0.96, $P = 0.000$), although *nosZ* showed a lower correlation (0.52, $P = 0.000$) (Fig. S4a). Abundances of *narG* and *napA* were highly correlated (Spearman's rho = 0.92, $P = 0.000$), as well as abundances of *nirS* and *nirK* (Spearman's rho = 0.94, $P = 0.000$). However, relative abundances of *narG* and *napA* were negatively correlated (Spearman's rho = −0.55, $P = 0.000$) (Fig. S4b). AOB and AOA (the

ammonia-oxidizing bacteria and archaea harbouring the *amoA* gene) showed very sparse distributions. Although AOB was a magnitude order more abundant (up to 1700 copies) than AOA, their abundances were moderately correlated (Spearman's rho = 0.50, $P = 0.000$). Few significant relationships involving environmental variables and genes distribution were found (Table S4). The few significant correlations involved complex relationships. For example, the relative abundance of *nosZ* was significantly, although negatively, correlated with pH, and not correlated with TN (Fig. S4c), even when TN which was in turn negatively correlated with pH (Table S1). Other significant correlations showed negative low values, like those between pH and abundances of 16S rRNA gene Bacteria and Archaea, *narG*, *napA*, *nirS* and *nirK*, and the relative abundance of *nirK*. pH also showed a significant and positive correlation with the abundance ratio *nosZ*/*narG*. Nitrate was significantly although low correlated with the abundance ratio *nirS*/*nirK* (Fig. S4d). TN was correlated with the relative abundance of *nirK*. Neither soil moisture nor TOC showed significant correlations with genes distribution. For ammonia-oxidizing communities, only *amoA* from AOA showed a significant correlation with ammonia (Spearman's rho = 0.41, $P = 0.02$). Vegetation cover showed low but significant correlations with total bacterial and crenarchaeal communities, and with absolute abundances of denitrifier genes *narA*, *napA*, *nirS* and *nirK*, but not with *nosZ*. However, the ratio between abundances of *nosZ*/*narG* showed a significant correlation. Only the relative abundance of *nirS* showed significant correlations with vegetation cover.

Total bacteria community determined by the 16S rRNA gene did not show a characteristic spatial dependence (Table S2 and Fig. S5a). In contrast, the abundance of the crenarchaeal community showed a characteristic spatial dependence, although over a scale around 10 m (Table S2). Relative abundances of *narG*, *napA*, and *nirS*, as well as the ratio *nirS*/*nirK*, showed spatial dependence at 8–11 m while it ranged near the limit of the sampled area (32 m) for the relative abundance of *nosZ* (Fig. 3 and Table S2). In contrast, the relative abundance of *nirK* showed no spatial dependence over the sampled area (linear model). Similarly, *nosZ* showed no characteristic spatial dependence (linear model) over the sampled area, while its relative abundance (*nosZ*/16S rRNA gene bacteria) showed spatial dependence at ranges near the limit of the sampled area (32 m). As *amoA* from bacteria and crenarchaea showed very sparse distributions, semivariograms could not be calculated.

Fractal variograms of abundances and relative abundances of genes showed a general trend towards repetitive plane distributions, but only abundance of *nirK*, relative abundances of *nirS*, *nirK*, *nosZ* and the ratio *nirS*/*nirK* showed a good fit (D between 1.68 and 1.93, R^2 between 0.57 and 0.89, Table S3).

Interpolated (kriged) maps of genes distribution showed in general a poor fit, except for the total crenarchaeal community and the relative abundance of *nosZ* (Table S3). Spatial distribution of genes is shown in Fig. 4 and Fig. S6. As *amoA* from bacteria and Crenarchaea showed very sparse distributions, kriged maps could not be fitted. A quantile post diagram is shown for

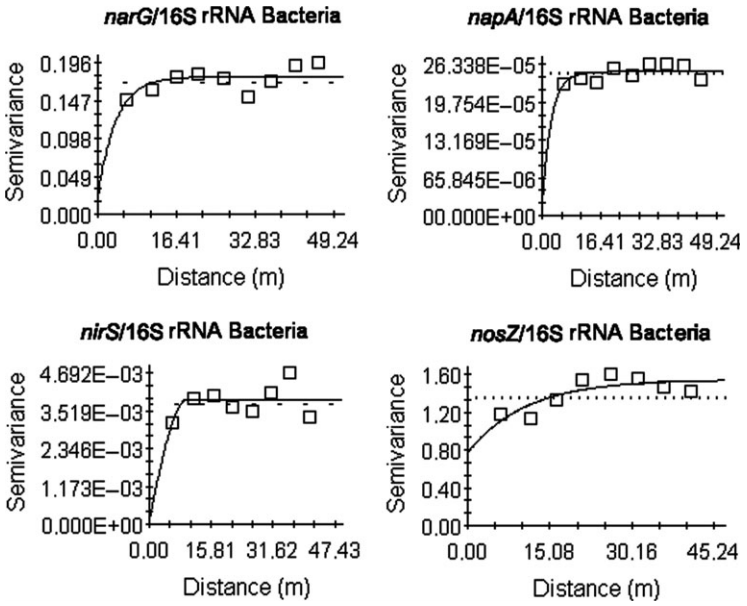

Fig. 3. Semivariograms of some denitrification genes (relative abundances to total bacterial community). Semivariance models and parameters for all the studied genes are given in Table S2.

AOA (Fig. S7a), together with the kriged map for ammonia distribution (Fig. S7b).

Denitrification activity and products

Potential denitrification activity (DEA), potential N_2O production, and the proportion of terminal N_2O produced as terminal product of denitrification [$N_2O/(N_2O + N_2)$] showed highly heterogeneous distributions over the sampled area. DEA varied from sampling sites with no activity to 600 ng N-N_2O g^{-1} dry soil h^{-1}. Potential N_2O production also varied widely, from no production to 22.41 ng N-N_2O g^{-1} dry soil h^{-1}.

As expected, denitrification variables were significantly correlated between them and also showed correlations with some environmental variables in a complex way (Table S1). DEA was negatively correlated with pH and positively correlated with TOC and TN, although not with nitrate. It was also correlated with potential N_2O production and negatively correlated with $N_2O/(N_2O + N_2)$. Potential N_2O production showed a similar correlation pattern with other variables as DEA. Denitrification activity variables (DEA and potential N_2O production) were similarly correlated although with relatively low values with vegetation cover. As showed in Table S4, DEA and potential N_2O production were similarly correlated although with relatively low values with total bacterial and crenarchaeal communities, and with abundances of *narG*, *napA*, *nirK*, *nirS*/*nirK*. However, DEA and potential N_2O production showed no correlations with *nosZ*. Relative abundances of *nirS* and *nosZ* showed similar significant correlations with DEA, while relative abundances of *nirS* and *narG* similarly correlated with potential N_2O production. In contrast, the $N_2O/(N_2O + N_2)$ ratio did not show correlation with any absolute or relative gene abundance.

Denitrification variables showed a characteristic spatial dependence over small ranges (between 7 and 10 m), as revealed by the fitted semivariance models (Table S2). However, DEA and potential N_2O production showed a peak in spatial dependence around 24 m, not present in the $N_2O/(N_2O + N_2)$ ratio (Fig. 5).

Fractal variograms showed *D* values close to 2, indicating a plane distribution of self-similar, repetitive variation of the denitrification variables over the sampled area, but with relatively low fit (R^2 from 0.33 to 0.60, Table S3).

Interpolated (kriged) maps of denitrification variables distribution showed a good fit only for DEA (Fig. 6, Table S3).

Discussion

In this work, we studied the spatial pattern of N-cycle processes and communities in a constructed wetland with a seasonal flooding water regime, in relation with environmental variables (sediment biogeochemical properties and vegetation cover). Biogeochemical properties of the sediments showed contrasted spatial distributions. Both pH and sediment moisture showed autocorrelation patterns over larger scales (around 30 m) compared with

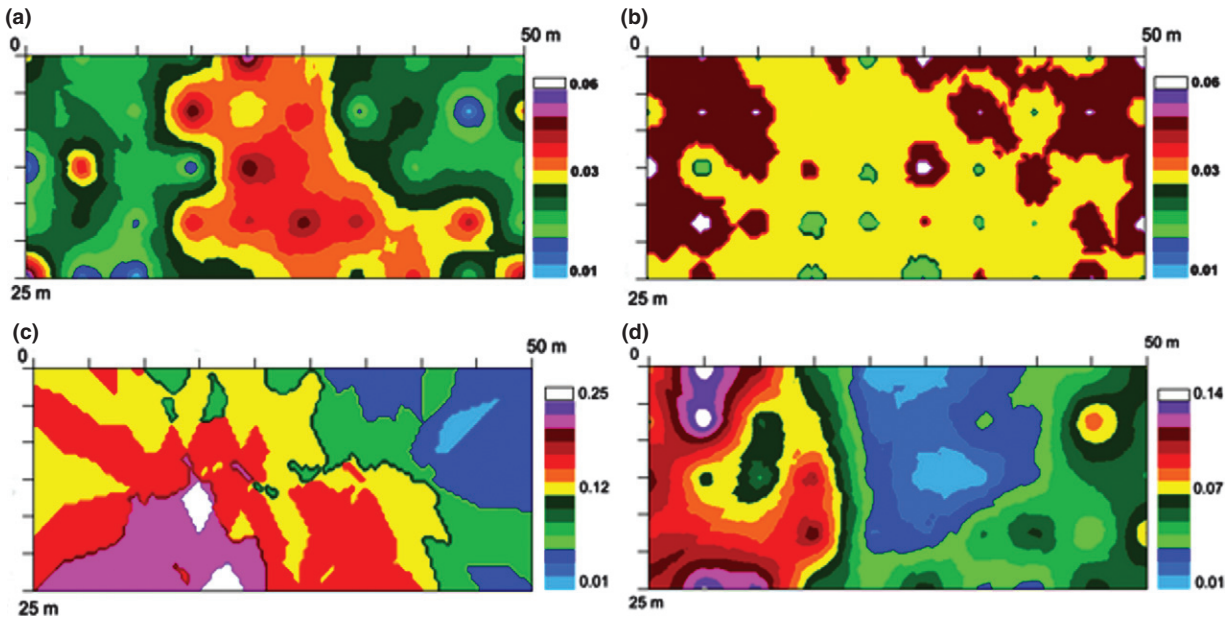

Fig. 4. Interpolated maps for some gene relative abundances distributions. (a) *narG*, (b) *napA*, (c) *nirS* and (d) *nosZ*. Colour scales indicate extrapolated values by kriging. Maps are shown in the same orientation as in Fig. S1b (sampling area).

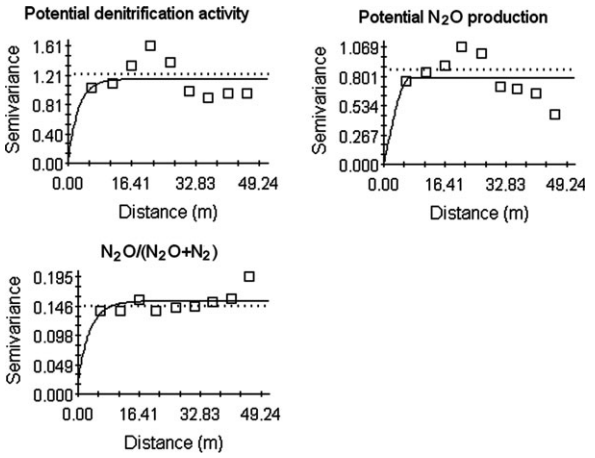

Fig. 5. Semivariograms of denitrification variables. Semivariance models and parameters are given in Table S2.

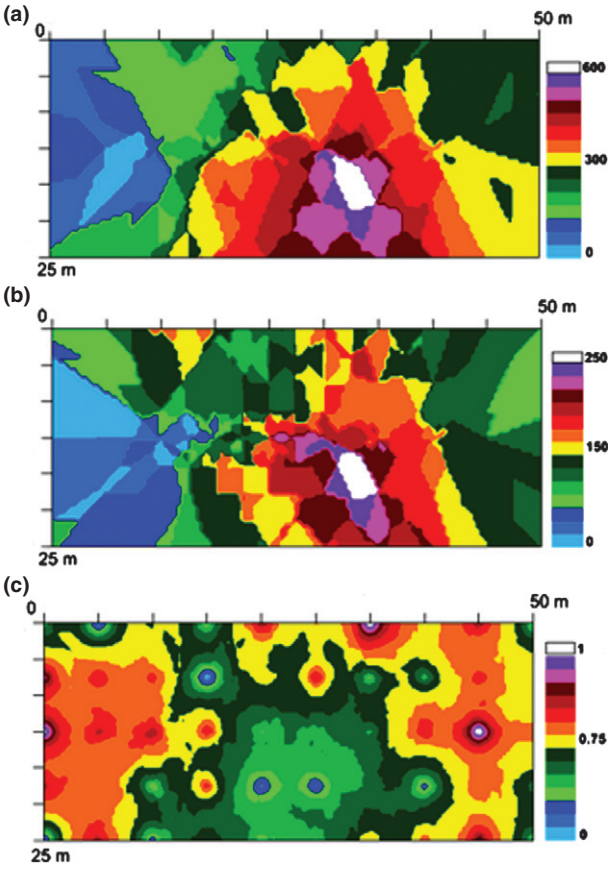

Fig. 6. Interpolated maps for denitrification variables distributions. (a) Potential denitrification activity (DEA), (b) potential N_2O production, (c) $N_2O/(N_2O + N_2)$. Colour scales indicate extrapolated values by kriging. Maps are shown in the same orientation as in Fig. S1b (sampling area).

total organic carbon, nitrate and ammonia contents (around 8–10 m). Total nitrogen content showed autocorrelation over the entire sampled area. Thus, over the scale considered in the study, almost no patchiness was found for pH and sediment moisture, while smaller scale patchiness was found for carbon, nitrate and ammonia.

Both DEA and potential N_2O production had a common spatial pattern with lower rates north-west of the wetland and highest rates in the central area. This pattern was markedly different to that of the $N_2O/(N_2O + N_2)$ ratio, which showed the highest ratios in the middle of the wetland. This was supported by the significant negative correlation between DEA and the $N_2O/(N_2O + N_2)$ ratio, which suggests that N_2O is more reduced in areas where the potential denitrification is higher. Similar results were reported in a pasture soil by Philippot *et al.* (2009a), who showed that the spatial patterns of soil properties, which were strongly affected by presence of cattle, imposed significant control on potential denitrification activity and potential N_2O production.

It is well-known that denitrification highly depends on soil variables like pH, water content, N amount and forms present, and available carbon (Groffman *et al.*, 1988). However, we found low or no correlations of denitrification with pH, sediment moisture and nitrate, and only low correlations with organic carbon, nitrogen and vegetation cover. Although in the wetland system studied the potential denitrification activity and the potential N_2O production weakly depended on some environmental properties and microbial communities, the proportion of the final products of denitrification, either N_2 or N_2O, did not depend on the variables studied, although indeed showed a defined spatial pattern. An inverse relationship between pH, the relative abundance of *nosZ* and the proportion N_2O as terminal product of denitrification was found by Philippot *et al.* (2009a). We found a negative relationship between pH and the potential N_2O production but not relationship between pH and the relative abundance of *nosZ*, nor with the proportion N_2O as terminal product of denitrification. It is known that a low pH increases N_2O production from denitrification (Šimek *et al.*, 2004) through a decrease in N_2O reduction (Van den Heuvel *et al.*, 2011), and thus, our result is difficult to explain.

The spatial distribution of N-cycling microbial communities of constructed wetland sediments from crop irrigation waters was heterogeneous and complex. Total communities of bacteria and crenarchaea showed different spatial distributions, with no characteristic spatial dependence over the sampled area for the 16S rRNA gene of bacteria, but with spatial autocorrelation at small scales for the 16S rRNA gene of crenarchaea. Genes involved in the nitrification and denitrification processes were distributed following spatial patterns with different

degrees of autocorrelation but in general confined to small distances, around 10 m. Analysis of autocorrelation patterns through semivariance and fractal variograms indicated a tendency to a patchy distribution over small scales.

Given the limited availability of comparable published works on N-cycling genes distribution focusing constructed wetlands and on small spatial scales, discussion of our results is somewhat limited to previous works made on soils, mainly grasslands and farms. Philippot *et al.* (2009a) reported in grazed grasslands a nonrandom distribution pattern of the size of the denitrifier community estimated by quantification of the denitrification genes copy numbers with a scale spatial dependence (6–16 m) similar to that found in our work. Keil *et al.* (2011) found, also in grasslands, that soil properties were affected by management practices and showed spatial heterogeneity on greater scales compared with gene distributions. The discrepancy we found between the spatial distributions of environmental variables such as pH and sediment moisture and genes could be responsible for the few associations found between their respective spatial patterns. However, even in the case of sediment biogeochemical properties showing spatial organization at smaller scales (TOC, nitrate and ammonia) comparable with that of the genes, a consistent pattern of relationship with genes did not appear in our study. A few more correlations appeared between denitrification variables (DEA and potential N_2O production) and some gene distributions. Vegetation cover correlated with pH and almost all absolute gene abundances, only with relative abundances of *nirS* and *nosZ*, and with DEA and potential N_2O production. However, all the correlations found with vegetation showed relatively low values. This is unexpected because the fluxes of N_2O in a Danish wetland were influenced by gas transport mediated by macrophytes (Jørgensen *et al.*, 2011). These findings configure a scenario of complex relationships between spatial distributions of biogeochemical properties of the sediments, genes and denitrification activities and products, dominated more by specific correlations than by a general pattern. This general decoupling of spatial organization of habitat variables and genes was shown also by the mentioned comparable studies. Philippot *et al.* (2009a) found that the spatial patterns of soil properties did not influence the size of the denitrifier community. Keil *et al.* (2011) found that spatial heterogeneity decreased with higher grassland use including fertilization for soil biogeochemical properties, but increased for N-cycling microorganisms, allowing the authors to think that factors not considered in the study were driving the microbial distribution found. Even when sampling was performed using a nested scale approach, from cm to m, only a few significant correlations were found (Keil *et al.*, 2011). Thus, reducing the sampling scale to cm did not render further strong evidence of correlation between spatial patterns of soil properties and N-cycling microbial communities. Regarding the spatial distribution of microbial communities, probably the adequate scale could be even smaller. Nunan *et al.* (2002) found aggregated pattern of microbial communities in an arable soil using geostatistics, with lengths of spatial autocorrelation varying between 240 and 1560 μm in the topsoil and 0–990 μm in the subsoil. It is also possible to think that a scale issue may be involved, not only related with two dimensional but also with the three-dimensional distribution of microbial communities in soil (wetland sediment in our work). For example, Dechesne *et al.* (2003) studied the spatial distributions of ammonia oxidizers and 2,4-D degraders microbial communities using a 3D experimental and modelling approach considering different volume scales (from 50 μm^3) and found different 3D aggregated spatial distributions of the two microbial groups. This differential distribution might have been related with the distribution of the substrate (ammonia or 2,4-D) through the complex 3D pattern of soil pores (Dechesne *et al.*, 2007).

Although in our work a general pattern of spatial correspondence between sediment properties and N-cycle-associated microbial communities did not appear at the sampling scale used, clearly the distribution of the microbial communities associated with the N-cycle showed a heterogeneous, patchy pattern that in some cases suggests a differential utilization of the sediment habitat by microbial groups harbouring different genes implicated in similar paths of the denitrification process. For example, although both *narG* and *napA* genes [coding for membrane-bound and periplasmic nitrate reductase, respectively, harboured by the same or different bacteria (Deiglmayr *et al.*, 2004)] code for the same step in denitrification, their relative abundances were negatively correlated. Moreover, the relative abundance of these two genes showed larger patches for *narG* (higher range of autocorrelation length), as shown in the interpolated maps. Thus, microbial groups harbouring *narG* or *napA* occupy differential habitat locations perhaps reflecting past competitive exclusion. Relative abundances of *nirS* and *nirK* genes [coding for cytochrome cd_1 or copper nitrite reductase, respectively, also carried by different bacteria (Jones *et al.*, 2008)] were not correlated, in spite of the apparently similar distributions of absolute abundances of *nirS* and *nirK* shown by the interpolated maps. This may be due to their very different absolute abundance ranges (*nirS* was an order of magnitude more abundant than *nirK*). The distribution of the relative abundances of these two genes indicates that bacterial

groups harbouring *nirS* are much more abundant than those carrying *nirK* and that they may use the habitat differentially but not exerting competitive exclusion. Our findings agree in general with results from other works studying the spatial distribution of *narG*, *napA*, *nirS* and *nirK* genes, showing differential habitat use by bacteria harbouring genes coding for the same denitrification step (Hallin *et al.*, 2009; Philippot *et al.*, 2009a; Enwall *et al.*, 2010; Keil *et al.*, 2011). As genes in both functionally redundant pairs (*narG-napA* and *nirS-nirK*) showed the same correlation pattern with the environmental variables considered in this study, it is clear that some other dimension of the ecological niche may be explaining the different spatial distribution of bacteria carrying these genes. Among other relevant niche components, spatial distribution of nutrients and water adsorbed in the three-dimensional soil micro-structure, as well as interactions with other bacteria and predators (especially protozoa), is an important factor in determining the spatial distribution of soil bacteria (Dechesne *et al.*, 2007).

In contrast to the pairs, *narG-napA* and *nirS-nirK*, the genes encoding the first step of nitrification, *amoA*, from bacteria and archaea showed a moderate correlation, indicating that this nitrification step may be performed simultaneously by bacteria and archaea in the same habitat location. However, as spatial distribution of both AOA and AOB were highly sparse further interpretations in terms of possible ecological niche variables involved is difficult to make. Our results contrast with those found for the same gene by Wessén *et al.* (2011) in soils at farm scale, where spatial distributions of both communities did not overlap and were related with soil pH and clay content. In our study, AOB abundance was higher than AOA abundance, as shown also by Tada *et al.* (2011) and by Limpiyakorn *et al.* (2011) in constructed wetlands for wastewater treatment. However, we found that only AOA showed a significant correlation with ammonia in spatial locations of joint occurrence with ammonia. This may be explained by the finding of Limpiyakorn *et al.* (2011) that AOA can outcompete AOB under low ammonium levels, comparable to those found in our study.

Coming back to our formulated hypothesis, we found a mixed support to it, because the spatial distribution of N-cycle-associated microbial communities and genes, and their functional activities, showed a complex relationship with wetland sediment properties and environmental variables. Microbial genetic background is an important factor shaping the microbial niche, which may or not allow a bacterial group to exploit its microhabitat and even modify it (Marco, 2008). However, further studies involving a range of spatial scales, other potentially relevant niche dimensions like O_2 soil diffusion and also incorporating a three-dimensional approach could be useful to explain the seeming uncoupling between spatial distributions of environmental properties and those of microbial communities.

Acknowledgements

This study was supported by ERDF-cofinanced grants P09-RNM-4746 from Consejería de Economía, Innovación y Ciencia (Junta de Andalucía, Spain). D.C. is recipient of a predoctoral grant from MEC. D.E.M. is a member of the National Research Council (CONICET, Argentina) and thanks MEC for a Sabbatical Leave at Department of Soil Microbiology and Symbiotic Systems (Agencia CSIC, Granada, Spain).

References

Bachand PAM & Horne AJ (2000b) Denitrification in constructed free-water surface Wetlands: II. Effects of vegetation and temperature. *Ecol Eng* **14**: 17–32.

Bru D, Sarr A & Philippot L (2007) Relative abundance of the membrane bound and periplasmic nitrate reductase. *Appl Environ Microbiol* **73**: 5971–5974.

Bruland GL, Richardson CJ & Whalen SC (2006) Spatial variability of denitrification potential and related soil properties in created, restored, and paired natural wetlands. *Wetlands* **26**: 1042–1056.

Burrough PA (1981) Fractal dimensions of landscapes and other environmental variables. *Nature* **294**: 240–242.

Chon K, Chang J-S, Lee E, Lee J, Ryu J & Cho J (2011) Abundance of denitrifying genes coding for nitrate (*narG*), nitrite (*nirS*), and nitrous oxide (*nosZ*) reductases in estuarine versus wastewater effluent-fed constructed wetlands. *Ecol Eng* **37**: 64–69.

Craddock VM & Henderson AR (1986) Effect of N-nitrosamines carcinogenic for oesophagus on O^6-alkyl-guanine-DNA-methyl transferase in rat oesophagus and liver. *J Cancer Res Clin Oncol* **111**: 229–236.

Cressie NAC (1991) *Statistics for Spatial Data*, John Wiley & Sons, New York, NY.

Dechesne A, Pallud C, Debouzie D, Flandrois JP, Vogel TM, Gaudet JP & Grundmann GL (2003) A novel method for characterizing the microscale 3D spatial distribution of bacteria in soil. *Soil Biol Biochem* **35**: 1537–1546.

Dechesne A, Pallud C & Grundmann GL (2007) Spatial distribution of bacteria at the microscale soil, *In the Spatial Distribution of Microbes in the Environment* (Franklin RB & Mills AL, eds.), pp. 87–107. Springer, Dordrecht.

Deiglmayr K, Philippot L, Hartwig UA & Kandeler E (2004) Structure and activity of the nitrate-reducing community in the rhizosphere of *Lolium perenne* and *Trifolium repens* under long-term elevated atmospheric pCO_2. *FEMS Microbiol Ecol* **49**: 445–454.

Enwall K, Throbäck IN, Stenberg M, Söderström M & Hallin S (2010) Soil resources influence spatial patterns of

denitrifying communities at scales compatible with land management. *Appl Environ Microbiol* **76**: 2243–2250.

Garcia-Lledó A, Bañeras L, Ruiz-Rueda O, Vilar-Sais A & Sala L (2011) Plant coverage affects nitrogen removal efficiencies in a free water surface constructed wetland by microbial nitrification and denitrification activities. *Ecol Eng* **37**: 678–684.

Greer FR & Shannon M (2005) Infant methemoglobinemia: the role of dietary nitrate in food and water. *Pediatrics* **116**: 784–786.

Groffman PM, Tiedje JM, Robertson GP & Christensen S (1988) Denitrification at different temporal and geographical scales: proximal and distal controls. *Advances in Nitrogen Cycling in Agriculture Ecosystems*. (Wilson JR, ed.), pp. 174–191. CAB International, Wallingford.

Hallin S, Jones C, Schloter M & Philippot L (2009) Relationship between N-cycling communities and ecosystem functioning in a 50-year-old fertilization experiment. *ISME J* **3**: 597–605.

Henry S, Baudouin E, López-Gutiérrez JC, Martin-Laurent F, Brauman A & Philippot L (2004) Quantification of denitrifying bacteria in soils by *nirK* gene targeted real-time PCR. *J Microbiol Methods* **59**: 327–335.

Henry S, Bru D, Stres B, Hallet S & Philippot L (2006) Quantitative detection of the *nosZ* gene, encoding nitrous oxide reductase, and comparison of the abundances of 16S rRNA, *narG*, *nirK*, and *nosZ* genes in soils. *Appl Environ Microbiol* **72**: 5181–5189.

Hey DL, Kostel JA, Crumpton WG, Mitschand WJ & Scott B (2012) The roles and benefits of wetlands in managing reactive nitrogen. *J Soil Water Conserv* **67**: 47–53.

Jones CM, Stres B, Rosenquist M & Hallin S (2008) Phylogenetic analysis of nitrite, nitric oxide, and nitrous oxide respiratory enzymes reveal a complex evolutionary history for denitrification. *Mol Biol Evol* **25**: 1955–1966.

Jørgensen CJ, Struwe S & Elberling B (2012) Temporal trends in N_2O flux dynamics in a Danish wetland – effects of plant-mediated gas transport of N_2O and O_2 following changes in water level and soil mineral-N availability. *Glob Change Biol* **18**: 210–222. In press. doi: 10.1111/j.1365-2486.2011.02485.x

Kallner Bastviken S, Eriksson PG, Martins I, Neto JM, Leonardson L & Tonderski K (2003) Potential nitrification and denitrification on different surfaces in a constructed treatment wetland. *J Environ Qual* **32**: 2414–2420.

Kandeler E, Deiglmayr K, Tscherko D, Bru D & Philippot L (2006) Abundance of *narG*, *nirS*, *nirK*, and *nosZ* genes of denitrifying bacteria during primary successions of a glacier foreland. *Appl Environ Microbiol* **72**: 5957–5962.

Keil D, Meyer A, Berner D *et al.* (2011) Influence of land-use intensity on the spatial distribution of N-cycling microorganisms in grassland soils. *FEMS Microbiol Ecol* **77**: 95–106.

Kjellin J, Hallin S & Wörman A (2007) Spatial variations in denitrification activity in wetland sediments explained by hydrology and denitrifying community structure. *Water Res* **20**: 4710–4720.

Klappenbach JA, Saxman PR, Cole JR & Schmidt TM (2001) rrndb: the ribosomal RNA operon copy number database. *Nucleic Acid Res* **29**: 181–184.

Leonard M & Swanson GW III (2001) Comparison of operational design criteria for subsurface flow constructed wetlands for wastewater treatment. *Water Sci Technol* **43**: 301–307.

Limpiyakorn T, Sonthiphand P, Rongsayamanont C & Polprasert C (2011) Abundance of *amoA* genes of ammonia-oxidizing archaea and bacteria in activated sludge of full-scale wastewater treatment plants. *Bioresour Technol* **102**: 3694–3701.

Lopez-Gutiérrez JC, Henry S, Hallet S, Martin-Laurent F, Catroux G & Philippot L (2004) Quantification of a novel group of nitrate-reducing bacteria in the environment by real time PCR. *J Microbiol Methods* **57**: 399–407.

MAPA (1974) Métodos Oficiales de Análisis de Suelos y Aguas. Ministerio de Agricultura (Spain).

Marco D (2008) Metagenomics and the niche concept. *Theory Biosci* **127**: 241–247.

Nunan N, Wu K, Young IM, Crawford JW & Ritz K (2002) *In situ* spatial patterns of soil bacterial populations, mapped at multiple scales, in an arable soil. *Microbiol Ecol* **44**: 296–305.

Ochsenreiter T, Selesi D, Bonch-Ozmolovskaya L, Quaiser A & Schleper C (2003) Diversity and abundance of Crenarchaeota in terrestrial habitats studied by 16S RNA surveys and real time PCR. *Environ Microbiol* **5**: 787–797.

Park N, Kim JH & Cho J (2008) Organic matter, anion, and metal wastewater treatment in Damyang surface-flow constructed wetlands in Korea. *Ecol Eng* **32**: 68–71.

Peralta AL, Matthews JW & Kent AD (2010) Microbial community structure and denitrification in a wetland mitigation bank. *Appl Environ Microbiol* **76**: 4207–4215.

Petric I, Philippot L, Abbate C *et al.* (2011) Inter-laboratory evaluation of the ISO standard 11063 "soil quality – method to directly extract DNA from soil samples". *J Microbiol Methods* **84**: 454–460.

Philippot L, Cuhel J, Saby NPA, Chèneby D, Chronáková A, Bru D *et al.* (2009a) Mapping field-scale spatial patterns of size and activity of the denitrifier community. *Environ Microbiol* **11**: 1518–1526.

Philippot L, Bru D, Saby NPA, Cuhel J, Arrouays D, Simek M *et al.* (2009b) Spatial patterns of bacterial taxa in nature reflect ecological traits of deep branches of the 16S rRNA bacterial tree. *Environ Microbiol* **11**: 1518–1526.

Purkhold U, Pommerening-Roser A, Juretschko S, Schmid MC, Koops HP & Wagner M (2000) Phylogeny of all recognized species of ammonia oxidizers based on comparative 16S rRNA and *amoA* sequence analysis: implications for molecular diversity surveys. *Appl Environ Microbiol* **66**: 5368–5382.

Ramos C, Agut A & Lidón AL (2002) Nitrate leaching in important crops of the Valencian Community region (Spain). *Environ Pollut* **118**: 215–223.

Rockström J, Steffen W, Noone K *et al.* (2009) Planetary boundaries:exploring the safe operating space for humanity. *Ecol Soc* **14**: 32.

Ruiz-Rueda O, Hallin S & Bañeras L (2008) Structure and function of denitrifying and nitrifying bacterial communities in relation to the plant species in a constructed wetland. *FEMS Microbiol Ecol* **67**: 308–319.

Ryden JC & Dawson KP (1982) Evaluation of the acetylene-inhibition technique for the measurement of denitrification in grassland soils. *J Sci Food Agric* **33**: 1197–1206.

Šimek M, Elhottová D, Klimeš F & Hopkins DW (2004) Emissions of N_2O and CO_2,denitrification measurements and soil properties in red clover and ryegrass stands. *Soil Biol Biochem* **36**: 9–21.

Song K, Lee S-H, Mitsch WJ & Kang H (2010) Different responses of denitrification rates and denitrifying bacterial communities to hydrologic pulsing in created wetlands. *Soil Biol Biochem* **42**: 1721–1727.

Song K, Kang H, Zhang L & Mitsch WJ (2012) Seasonal and spatial variations of denitrification and denitrifying bacterial community structure in created riverine wetlands. *Ecol Eng* **38**: 130–134.

Sutton MA, Howard C, Erisman JW, Billen G, Bleeker A, Grenfelt P, van Grinsven H & Grizzetti B (Eds) (2011). *The European Nitrogen Assessment*. Cambridge University Press, Cambridge. 612 pp.

Tada C, Ikeda N, Nakamura S, Oishi R, Chigira J, Yano T, Nakano K & Nakai Y (2011) Animal wastewater treatment using constructed wetland. *JIFS* **8**: 41–47.

Tortosa G, Correa D, Sánchez-Raya AJ, Delgado A, Sánchez-Monedero MA & Bedmar EJ (2011) Nitrate contamination, biogeochemical properties and biological activities in surface waters and sediments of La Rocina stream (Doñana National Park, SW Spain): Greenhouse gas emissions and denitrification. *Ecol Eng* **37**: 539–548.

Treusch AH, Leininger S, Kletzin A, Schuster SC, Klenk HP & Schleper C (2005) Novel genes for nitrite reductase and *Amo*-related proteins indicate a role of uncultivated mesophilic crenarchaeota in nitrogen cycling. *Environ Microbiol* **7**: 1985–1995.

Van den Heuvel RN, Bakker SE, Jetten MSM & Hefting MM (2011) Decreased N_2Oreduction by low soil pH causes high N_2O emissions in a riparian ecosystem. *Geobiology* **9**: 294–300.

Vymazal J (2011) Constructed wetlands for wastewater treatment: five decades of experience. *Environ Sci Technol* **45**: 61–69.

Wessén E, Söderström M, Stenberg M *et al.* (2011) Spatial distribution of ammonia-oxidizing bacteria and archaea across a 44-hectare farm related to ecosystem functioning. *ISME J* **5**: 1213–1225.

Supporting Information

Additional Supporting Information may be found in the online version of this article:

Fig. S1. Study site at the constructed wetland (Los Guayules, Doñana National Park, South West Spain), showing the plant community (a) and sampling design (b).
Fig. S2. Vegetation cover of the sampled area. Cover percentage on a 25 cm × 25 cm square on each sample point was coded as 0 (no vegetation cover), 1 (1-50 % cover), 2 (51-75 % cover) and 3 (75-100 %) cover.
Fig. S3. Spatial distribution (kriged) maps for sediment moisture (%) and total organic carbon (g kg^{-1} dry sediment). Colour scales indicate extrapolated values.
Fig. S4. Some relationships found between genes and environmental variables. (a) Gene abundances, (b) gene relative abundances, (c) pH, Total Nitrogen and relative abundance of *nosZ* gene and (d) potential denitrification activity (DEA), nitrate concentration and abundance ratio *nirS*/*nirK* genes.
Fig. S5. Semivariograms of absolute abundances of total bacterial and archaeal communities (a) and some denitrification genes (a,b). Semivariance models and parameters for all the studied genes are given in **Table S3**.
Fig. S6. Spatial distribution (kriged) maps for denitrification genes (number of gene copies per ng sediment DNA). Colour scales indicate extrapolated values.
Fig. S7. Spatial variation of (a) *amo*A genes from AOA (number of gene copies per ng sediment DNA, quantiles), and (b) ammonia concentration (kriged map). Colour scales indicate extrapolated values.
Table S1. Correlations between biogeochemical properties of constructed wetland sediments, denitrification activity and products.
Table S2. Spatial analysis of environmental variables, gene abundances and activity of denitrifiers.
Table S3. Fractal variograms and interpolation (kriging) of environmental variables, gene abundances and activity of denitrifiers.
Table S4. Correlations between biogeochemical properties of constructed wetland sediments, N-cycling genes and denitrification activity.
Appendix S1. Statistical analyses.

Please note: Wiley-Blackwell is not responsible for the content or functionality of any supporting materials supplied by the authors. Any queries (other than missing material) should be directed to the corresponding author for the article.